JOURNAL OF CATALYSIS 90, 241–255 (1984)

Oscillations in Crystallite Shape during Heating in Hydrogen of Model Iron/Alumina Catalysts

I. SUSHUMNA AND E. RUCKENSTEIN[1]

Department of Chemical Engineering, State University of New York at Buffalo, Buffalo, New York 14260

Received April 16, 1984; revised July 5, 1984

Transmission electron microscopy is used to bring evidence for an alternation in the shape of iron crystallites supported on planar, nonporous, alumina substrates, when the specimens were heated, at 400°C, in hydrogen contaminated with traces of oxygen (less than 1 ppm) and/or moisture. The crystallites alternated between a torus which encloses a cavity and a shape in which an annular gap separates the torus from a core in the cavity. Electron diffraction indicated that this is accompanied by a corresponding alternation in the chemical state of the catalyst. The torus with an enclosed cavity corresponds to an oxidized state, in which iron oxides, resulting on oxidation by the contaminant oxygen, form solid solutions in alumina, with the tendency to approach the aluminates $FeAl_2O_4$ and/or $Al_2Fe_2O_6$. The torus containing a core in the cavity corresponds to a less-oxidized state, in which a part of the previously dissolved oxide diffuses out to be (at least partially) reduced by hydrogen to the metal and/or to a lower oxide (including possibly nonstoichiometric oxides). After prolonged heating, the two alternating shapes become less distinct, probably because of mechanical fatigue which eventually leads to a breakup of the crystallites. Similar behavior is observed at temperatures up to 600°C, though with diminished sharpness of the two alternating shapes above 500°C. An attempt is made to explain the shape alternation on the basis of surface phenomena resulting from the physical and chemical interactions between gas, crystallite, and substrate.

INTRODUCTION

Isothermal kinetic oscillations in heterogeneous catalytic systems have been studied extensively in recent years. Sheintuch and Schmitz (*1*) and Slin'ko and Slin'ko (*2*) have provided reviews on both the theoretical and experimental results. Periodic changes in reaction rates have been so far observed mostly during the oxidation of carbon monoxide and of hydrogen on Pt, Pd, and Ni wires, foils, and disks. Varghese *et al.* (*3*), Cutlip and Kenney (*4*), and Rathousky *et al.* (*5*) have reported oscillations during CO oxidation on supported Pt. Hlavácek and Rathousky (*6*) have reported chaotic behavior during CO oxidation on Pt supported on an alumina-coated-metal honeycomb matrix. In order to explain the oscillatory behavior, various mechanisms have been proposed, such as: coverage dependent activation energies (*7*), a change in reaction mechanism with surface coverage (*8*), alternative adsorption and desorption of a "poison" (inhibitor) present in traces in the reactant stream (*9*), and oxidation and reduction of the catalyst surface (*10*), to name a few. Though there is no agreement regarding the mechanism responsible, there is, however, a consensus that the coupling between the chemical and the transport rate processes, originally thought to give rise to these phenomena, is not the cause of the oscillations. Recent experiments seem to indicate that the behavior is rather a result of the physicochemical interactions between catalyst and reactants (and support where applicable). In order to associate the oscillations quantitatively with such interactions, the surface of the cata-

[1] To whom correspondence should be addressed.

0021-9517/84 $3.00

lyst should be monitored continuously for its changing chemical compositions. This is a difficult task. However, a qualitative correlation between the oscillatory behavior in the effluent concentration and the chemical and physical changes on the catalyst surface is possible. For instance, Kurtanjek *et al.* (*11*), in their experiments on hydrogen oxidation on Ni disks, performed contact potential difference (CPD) measurements and concluded that the oscillations were associated with the alternation of the catalyst surface between reduced and oxidized states. Recently, Sault and Masel (*12*) studied the same reaction on a Ni foil, employing a scanning Auger microprobe to characterize the surface. They observed that in all the cases in which oscillations were detected, only macroscopic protrusions of 5 to 20 μm were present on the surface of the catalyst. No such protrusions were however detected on the catalyst samples that did not give rise to oscillations. Within the resolution limit of their instrument (200–300 Å), they could not detect any submicrometer (microscopic) changes on the surfaces. In addition, there were no significant differences in the surface compositions of the catalyst samples which gave rise to oscillations and those which did not. Therefore, they concluded that the oscillations were caused by physical rather than chemical phenomena. Even though different origins have been suggested for the oscillations, Refs. (*11, 12*) indicate that the oscillations are associated with surface phenomena.

During experiments on oxidation–reduction behavior of different alumina-supported model catalysts, we observed, using transmission electronmicroscopy, that the iron crystallites supported on planar, nonporous, alumina substrates underwent oscillatory changes in shape during heating in hydrogen contaminated with traces of oxygen (less than 1 ppm) and/or moisture (less than 2 ppm). The crystallites changed their shape alternately between a torus with an enclosed cavity (Fig. 1a) and a shape in which an annular gap separates the torus from a core in the cavity. The latter shape is hereafter referred to as "core-and-ring structure" (Fig. 1b). Electron diffraction indicates that the shape alternation is accompanied by a corresponding alternation in the chemical state of the iron catalyst from an oxidized to a relatively reduced state. One could therefore expect that these shape alternations will be accompanied by detectable oscillations in the effluent concentration, when sufficiently large amounts of catalyst are used.

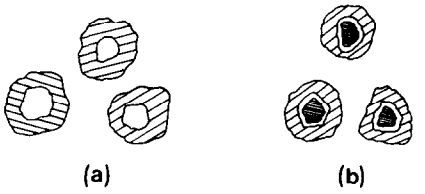

FIG. 1. Schematic of (a) torus and (b) core-and-ring structure.

EXPERIMENTAL

Electron-transparent, nonporous, alumina films of approximately 300 Å thickness, used as the support for the model catalysts, were prepared by anodization of chemically polished, high-purity aluminum foils by a technique described in (*13*). High-purity iron wire (99.998%, Alfa Products) was vacuum-evaporated onto alumina films supported on gold microscope grids, under a pressure of better than 2×10^{-6} Torr. The samples were heat-treated at atmospheric pressure inside a quartz tube 3.8 cm in diameter and 120 cm long. The flow rate of the gases was about 150 cm^3/min and was maintained constant during the heat treatment. The gases used in the experiments were all ultrahigh purity grade supplied by Linde Division, Union Carbide Corporation. Hydrogen and helium were both 99.999% pure, the former having less than 1 ppm O_2 and less than 2 ppm moisture and the latter having less than 3 ppm moisture. Prior to each heat treatment, the reactor was flushed with helium and the sample was heated in flowing helium until the pre-

set temperature was reached. Soon after the desired temperature was attained, helium was replaced by hydrogen and the latter was allowed to flow through the tube for a predetermined period of time. Subsequently, the sample was cooled down to room temperature in flowing helium, before being taken out for observation. After each heat treatment, the same regions of the sample were photographed using a JEOL, 100U transmission electron microscope.

RESULTS

Crystallites were generated in the model catalyst by heating the vacuum-deposited iron films in hydrogen. An alternation in the shape of the crystallites was observed both during the initial stages of crystallite formation as well as during further heating in hydrogen. It is important to note that hydrogen was used from the cylinder without further purification. It contained trace amounts of oxygen and/or moisture. Unless indicated otherwise, further use of the word "hydrogen" refers only to the above impure hydrogen. Experiments were carried out at different metal loadings to ascertain if the observed alternation in the shape of the crystallites was peculiar to a particular loading. The results were reproducible, though there were minor variations in behavior, probably due to small differences in sample preparation.

At 300°C, an initial iron film of about 6 Å thickness did not yield crystallites larger than 20 Å even after heating in hydrogen for 9 h, though a series of solid solutions of FeO (or possibly a nonstoichiometric oxide) in Al_2O_3, tending toward $FeAl_2O_4$, were detected by electron diffraction. [The formation of solid solutions was indicated by a gradual increase in the interplanar spacings (*d*-values), as measured by electron diffraction, from those of Al_2O_3, detected initially, to those of $FeAl_2O_4$ reached eventually. It is worth noting that the major *d*-values of the involved compounds are in the order FeO > $FeAl_2O_4$ > Al_2O_3 (FeO cannot be detected as a separate phase since it is unstable below 560°C).] At this loading, the temperature was probably too low to allow migration and coalescence of the initial small aggregates to form larger crystallites. For this reason, all the other experiments have been carried out at higher temperatures. Figure 2 shows selected results, at 400°C, for a sample having an initial film thickness of about 6 Å on crystalline alumina (sample A), while Fig. 3 shows results, at the same temperature, for a sample of about 12.5 Å initial film thickness on amorphous alumina (sample B). Since, as can be seen from Fig. 3, the particle density is already very high for a 12.5-Å film, higher loadings have not been investigated. Both samples exhibited oscillatory behavior in the shape of the crystallites. Sample A yielded a few crystallites on heating in hydrogen for 0.5 h. The particles were irregular in shape, nonuniform in size, and had a torus shape. As at 300°C, a solid solution of FeO in Al_2O_3, tending toward $FeAl_2O_4$ was detected, and, in addition, faint rings of γ-Fe_2O_3 (or Fe_3O_4) were also present. Note that, because γ-Fe_2O_3 and Fe_3O_4 have the same lattice constant, they cannot be differentiated by electron diffraction. Further heating in hydrogen, for consecutive short intervals of half an hour or an hour, brought about increases in particle size as well as modifications in the crystallite shape. The crystallites acquired a core in the cavity. The core then slowly disappeared and the crystallites returned to the torus shape. Two such additional shape alternations, observed on heating for longer time intervals, are shown in Fig. 2. After a few hours of heating, sample A contained two sets of solid solutions, one tending to form the lower aluminate, $FeAl_2O_4$, and the other to form the higher aluminate, $Al_2Fe_2O_6$. It is to be noted that the major *d*-values of the compounds are in the order: $Al_2Fe_2O_6$ > Fe_2O_3 ≈ Fe_3O_4. An increase in the major *d*-values from those of Fe_2O_3 toward those of $Al_2Fe_2O_6$ would indicate the formation of solid solutions of Fe_2O_3 in Al_2O_3 (or Al_2O_3 in Fe_2O_3), ultimately leading

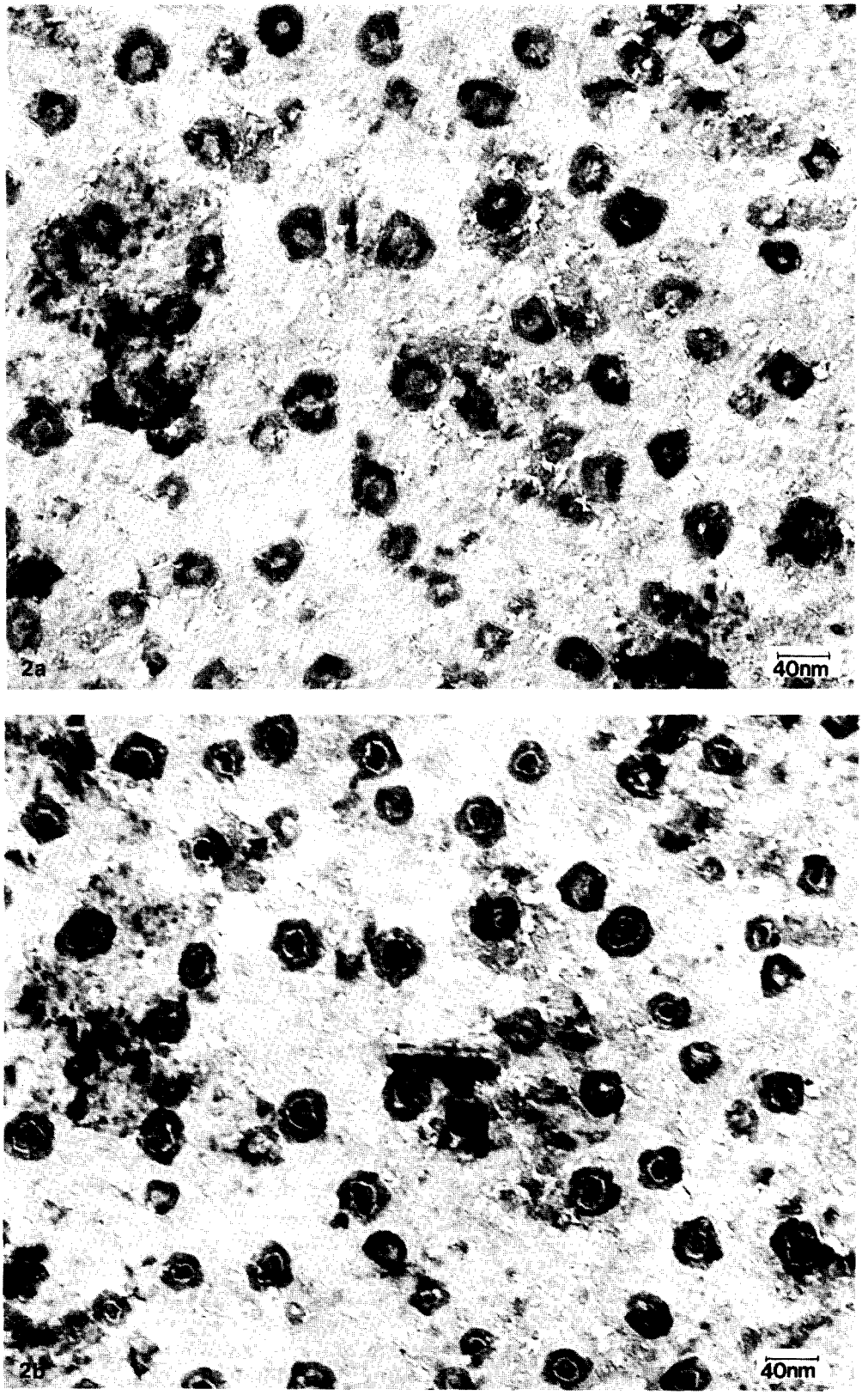

FIG. 2. Alternation in shape of crystallites on heating an iron on crystalline alumina specimen at 400°C in hydrogen contaminated with traces of oxygen and/or moisture. Initial film thickness: ~6 Å. The same regions are shown after a total of (a) 6 h, (b) 12 h, (c) 33 h, and (d) 36 h.

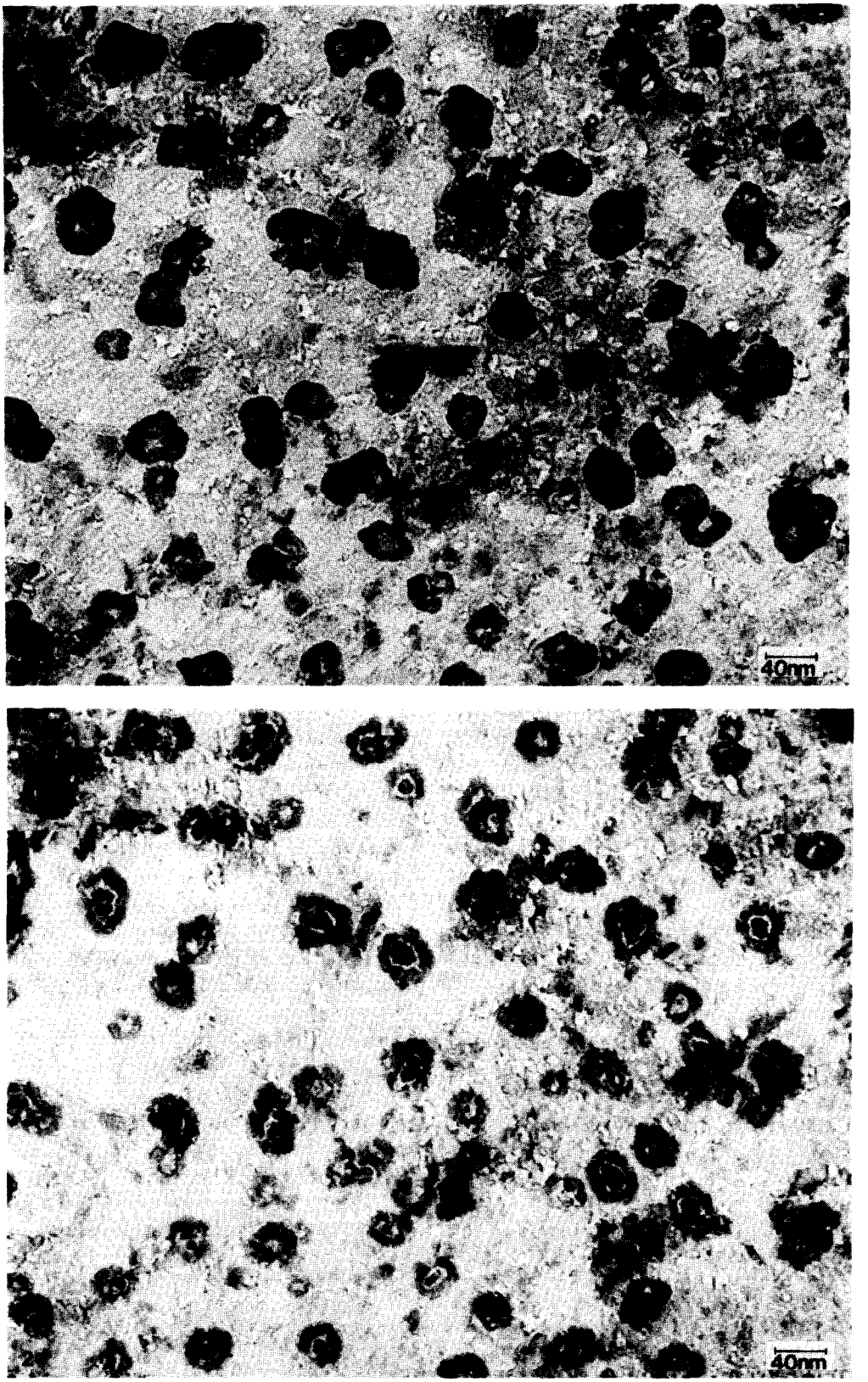

FIG. 2—*Continued.*

to the aluminate $Al_2Fe_2O_6$. A decrease in the *d*-values of one such solid solution toward those of Fe_2O_3 (or Fe_3O_4) would indicate partial precipitation of Fe_2O_3 from the solid solution and its eventual reduction to the metal and/or a nonstoichiometric lower oxide. However, an increase in the *d*-values toward those of $Al_2Fe_2O_6$ would indicate the formation of a greater amount of Fe_2O_3 and its subsequent dissolution in Al_2O_3. The latter state is considered to be an oxidized state, while the former a relatively reduced one.

Electron diffraction indicates that the torus shape in Fig. 2a is associated with the aluminate, $FeAl_2O_4$, and with a solid solution of Fe_2O_3 in Al_2O_3. A continuous heating for 6 h generated the core-and-ring structure shown in Fig. 2b. $FeAl_2O_4$, a solid solution of Fe_2O_3 in Al_2O_3 with *d*-values smaller than in the previous case, and metallic iron are now detected in the diffraction pattern. The core disappears on further heating. The micrograph shown in Fig. 2c, in which the torus shape is observed again, represents the state of the system after a total heating time of 33 h. The disappearance of the metal rings as well as an increase in the *d*-values of the solid solution of Fe_2O_3 in Al_2O_3 constitute the corresponding changes in the diffraction pattern, indicating oxidation. Figure 2d shows the micrograph taken when the specimen was heated for 3 additional hours. Faint metal rings are detected again in the diffraction pattern, in addition to the aluminate ($FeAl_2O_4$) and the solid solution of Fe_2O_3 in Al_2O_3.

Sample B, prepared with amorphous alumina and having a higher loading than sample A, was studied over a long period of time, up to 120 h, to check if the shape alternation continued indefinitely. (The background pattern due to the support is eliminated when the support is amorphous. For this reason, the use of amorphous alumina permits better resolution of the diffraction patterns and easier identification of the compounds.) Soon after deposition, even at room temperature, small crystallites very close to one another could be seen on the sample (Fig. 3a). On heating this sample for 1 h in hydrogen, interconnected islands were formed by the coalescence of the small crystallites (Fig. 3b). Electron diffraction indicated the presence of only Fe_3O_4 (or γ-Fe_2O_3). Two additional hours of heating led to the contraction and formation of less-interconnected islands, each island having a cavity or channel within it (Fig. 3c). During this heating, the *d*-values increased in comparison to those of Fe_2O_3, indicating the formation of a solid solution of Fe_2O_3 in Al_2O_3. Further heating increased the *d*-values gradually and also generated distinct islands. After a total of 21 h of heating, most of the crystallites were found to have the core-and-ring structure (Fig. 3d). In addition to a solid solution of Fe_2O_3 in Al_2O_3, α-iron could be detected. After a continuous heating for 6 additional hours, the particles are observed to be relatively extended over the surface and again channels and cavities, containing small residual particles, could be observed (Fig. 3e). The *d*-values increased further, tending toward those of $Al_2Fe_2O_6$. Another cycle of alternate shapes was observed upon further heating (Figs. 3f and g). Heating the specimen shown in Fig. 3g for half an hour led to the extension of the particles and also to a partial filling of the cavities (Fig. 3h). Mostly γ-Fe_2O_3 (or Fe_3O_4) could be detected by electron diffraction. This picture probably represents an intermediate stage of a transformation from the torus to the

FIG. 3. Sequence of changes on heating an iron on amorphous alumina specimen at 400°C in hydrogen contaminated with traces of oxygen and/or moisture. Initial film thickness: ~12.5 Å. The same regions are shown. (a) After deposition (b) 1 h; (c) 3 h; (d) 21 h; (e) 27 h; (f) 40 h; (g) 80 h; (h) 80 h, 30 min; (i) 81 h; (j) 81 h, 30 min; (k) 82 h; (l) 97 h; (m) 98 h; (n) 99 h; (o) 100 h, 30 min; (p) 118 h. Additional heating at 500°C for (q) 2 h; (r) 12 h; additional heating at 600°C for (s) 2 h and (t) 6 h.

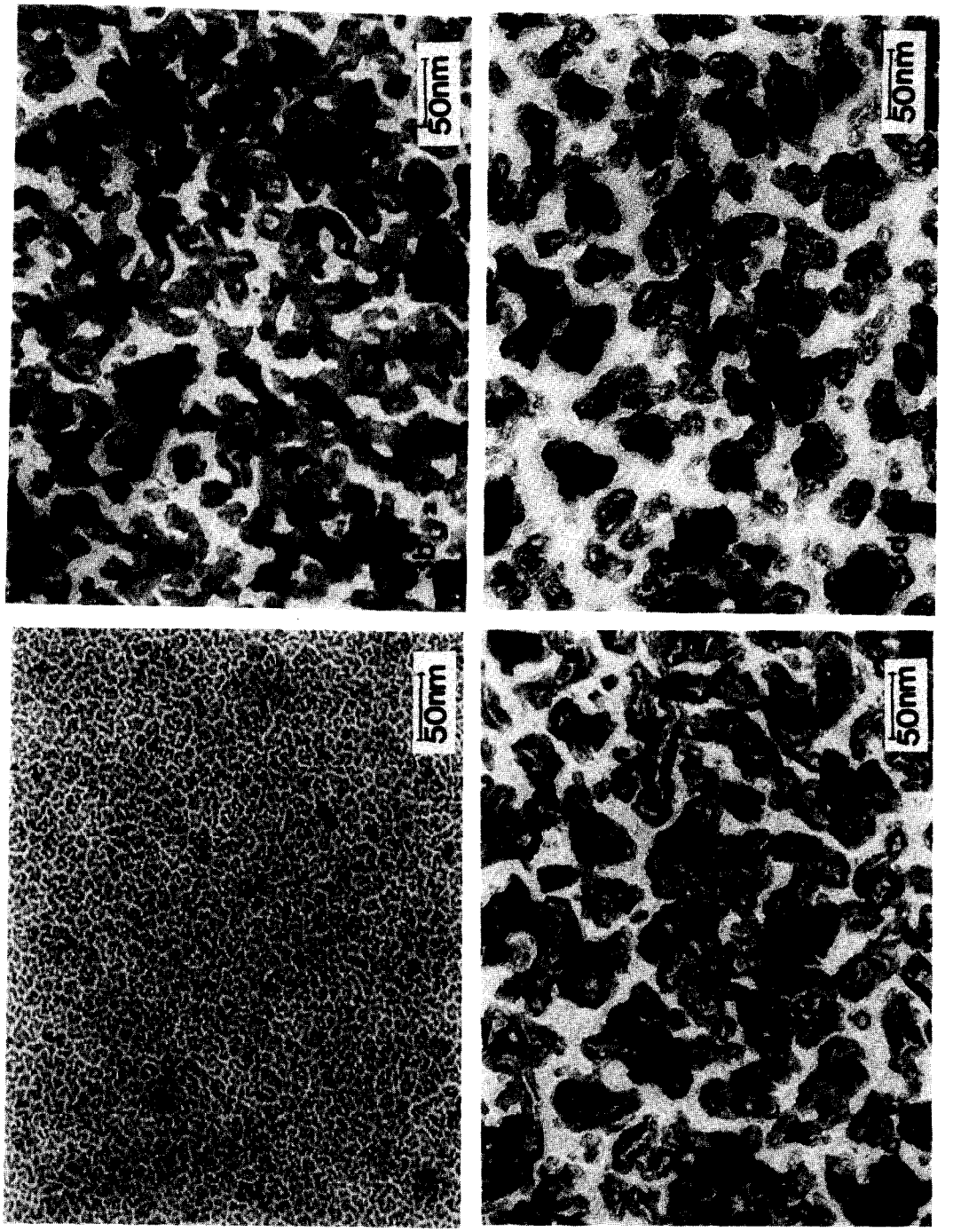

FIG. 3

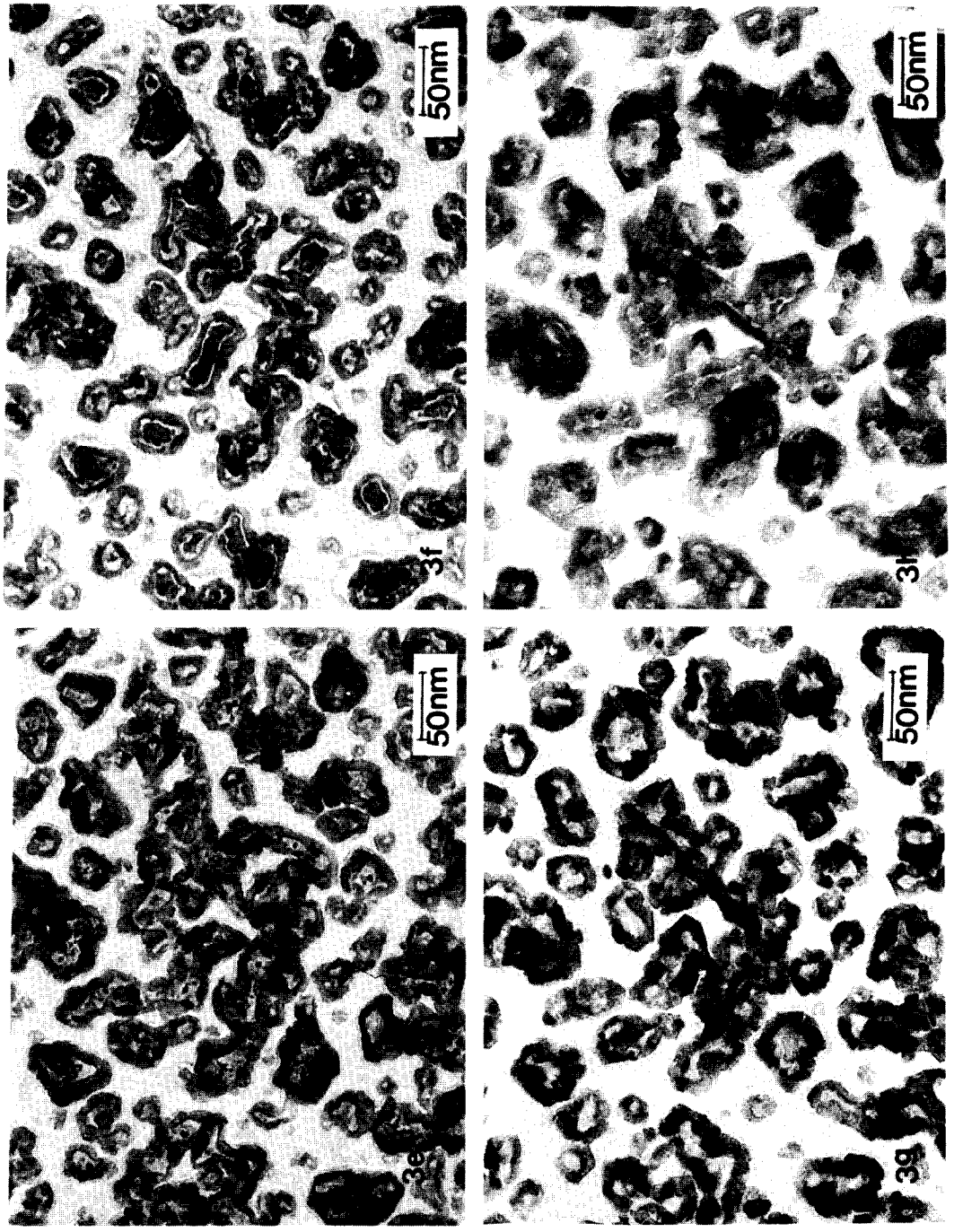
50nm
3f
50nm
3h
50nm
3e
50nm
3g

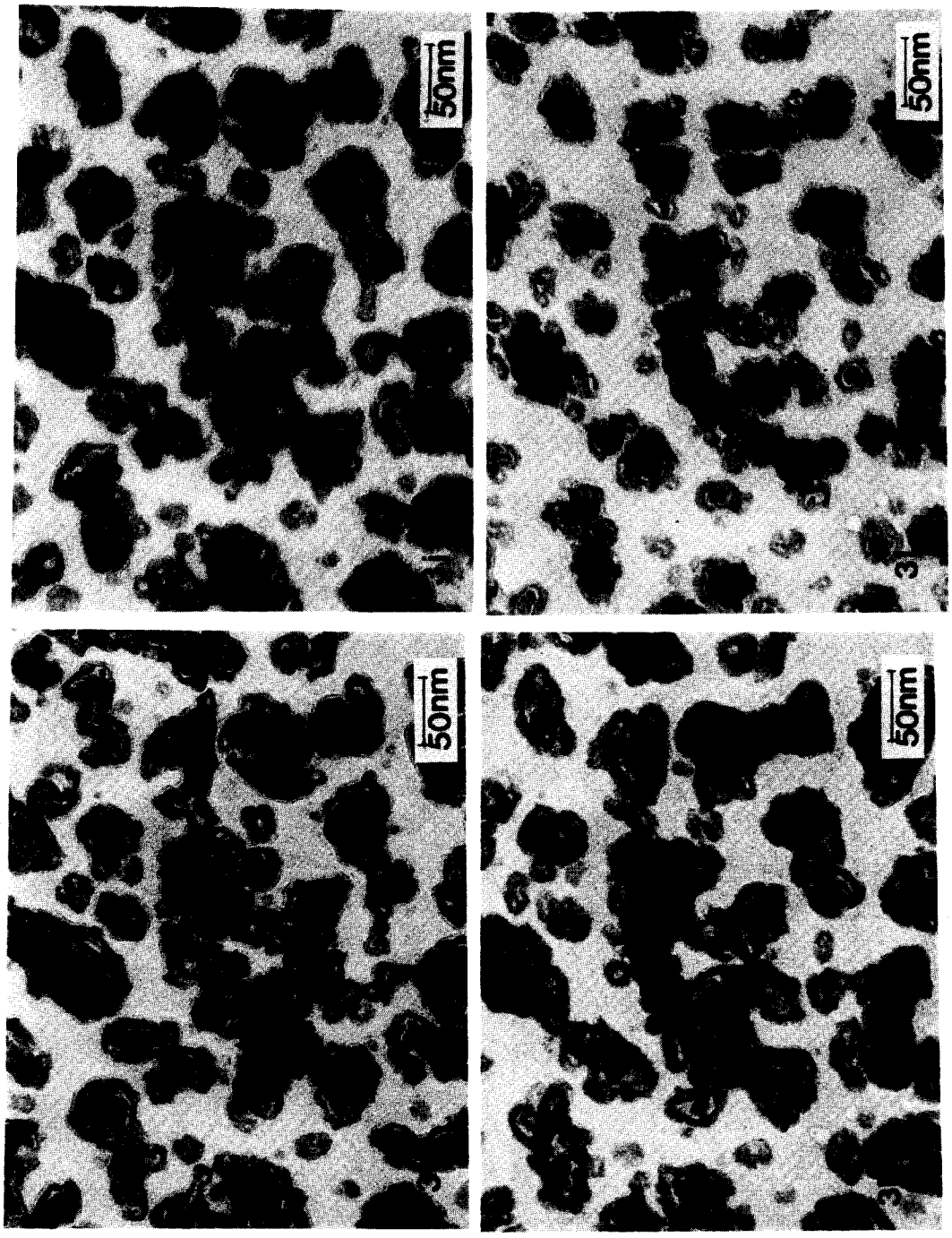

FIG. 3—*Continued.*

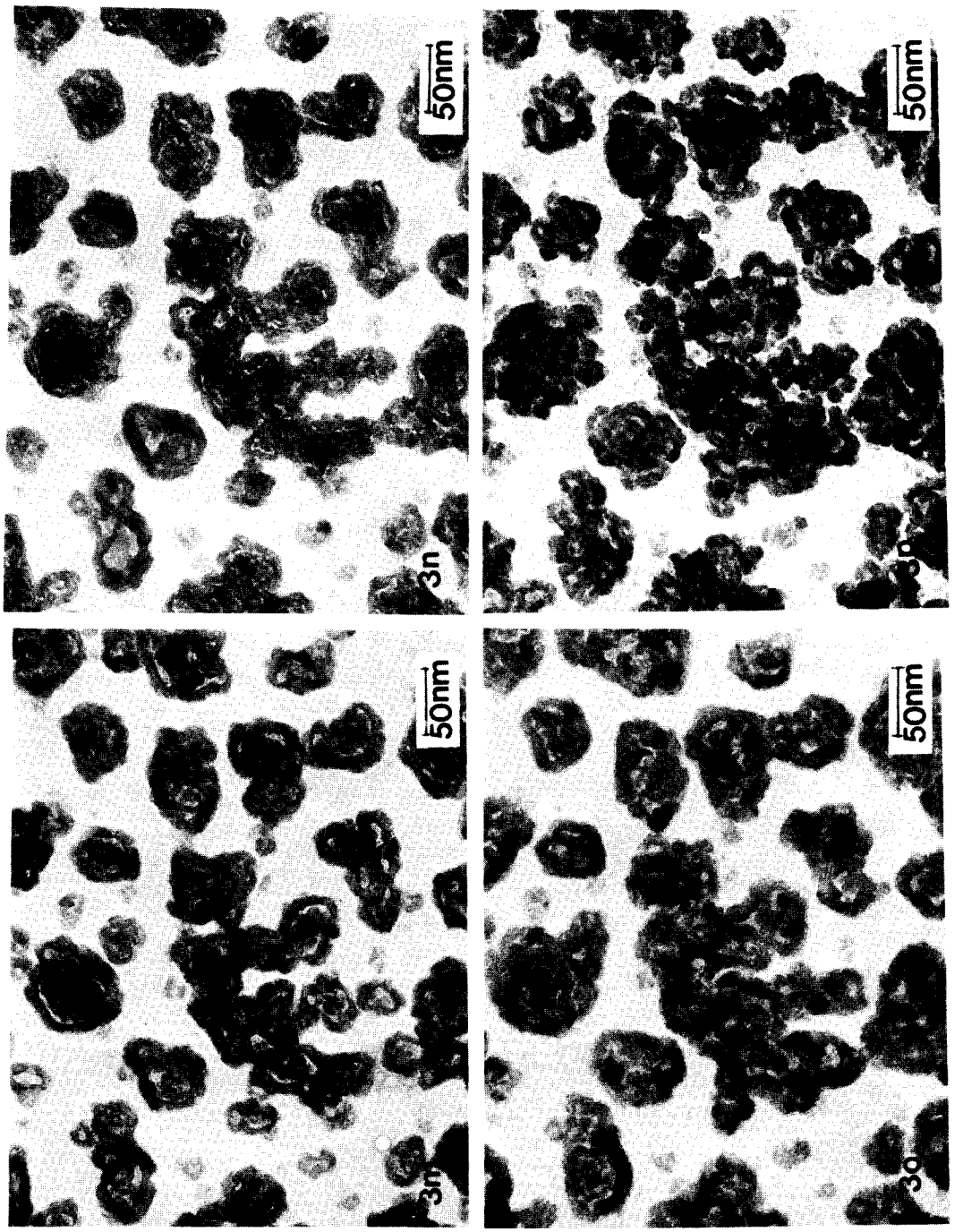

FIG. 3—*Continued.*

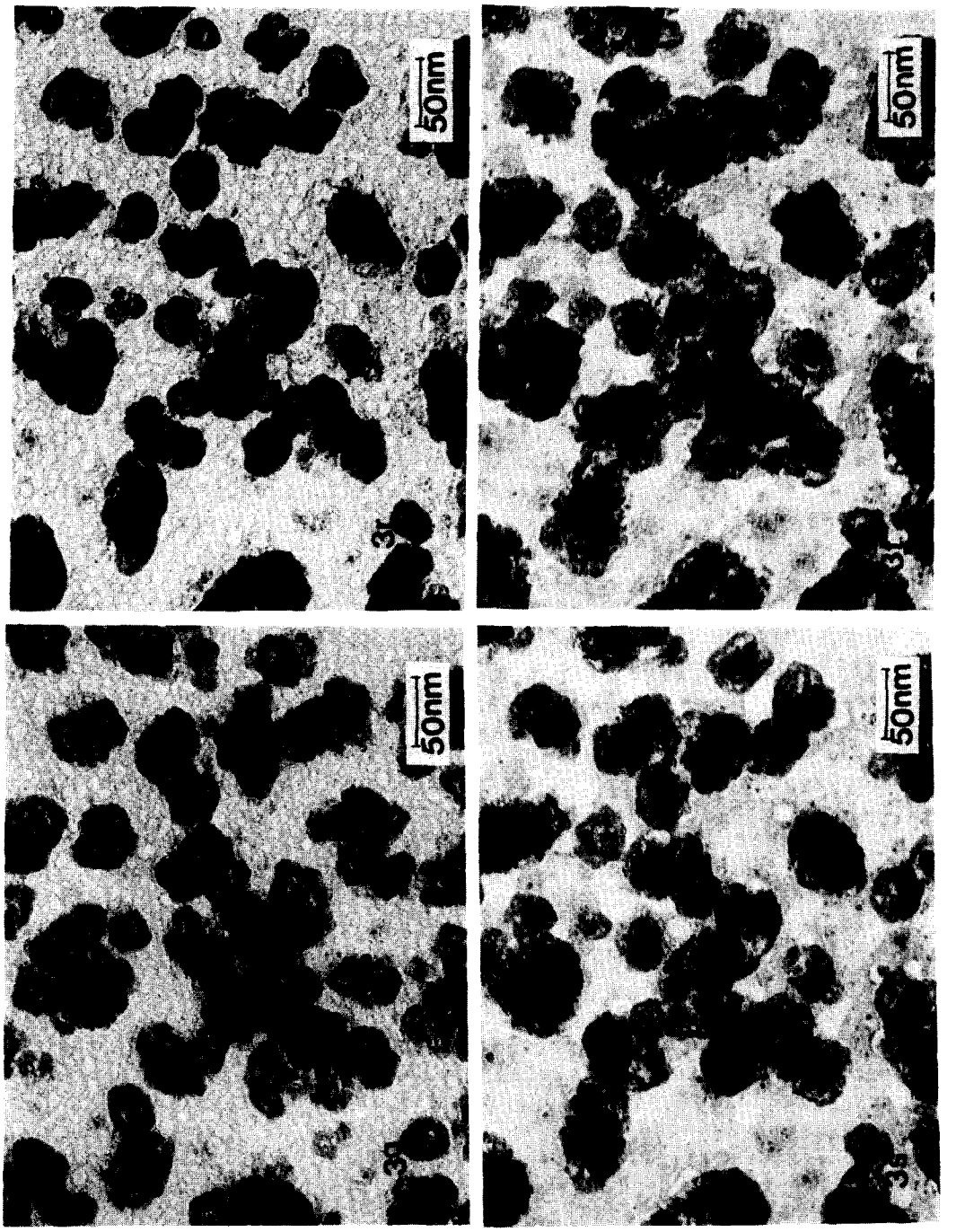

FIG. 3—*Continued.*

core-and-ring structure, or vice versa. After another half an hour of heating, some of this oxide was reduced to metal and the initiation of the core-and-ring structure could be observed (Fig. 3i). Electron diffraction indicated the presence of mostly γ-Fe_2O_3 (or Fe_3O_4) and some α-Fe.

One may note that the solid solution of Fe_2O_3 in Al_2O_3 exists both during the reduction step as well as during the oxidation step. It appears that during the oxidation step, the initially formed oxide diffuses into the substrate tending, via a succession of solid solutions, to form finally $Al_2Fe_2O_6$. During reduction, Fe_2O_3 diffuses back to the interface where at least a part is reduced to the metal. The torus shape is thus associated with an oxide and/or a solid solution which is tending toward $Al_2Fe_2O_6$. In contrast, the core-and-ring structure is associated with metal, γ-Fe_2O_3 (or Fe_3O_4), and a solid solution of Fe_2O_3 in Al_2O_3. The formation of $Al_2Fe_2O_6$ from Fe_2O_3 and Al_2O_3 as well as the reverse process do not necessarily have to be completed for the torus and the core-and-ring structure to be observed.

Shape alternation repeated during further heating, but the two alternating shapes were no longer as distinct as before, indicating the onset of a sluggish behavior (Figs. 3j to o). Further heating led to a breakup of the particles, which appear to be composed of a number of subunits (Fig. 3p). Electron diffraction indicated the presence of a solid solution with its *d*-values close to those of $Al_2Fe_2O_6$. Subsequent heating of the same sample in flowing oxygen for 1 h affected neither the composition of the catalyst, nor the shape of the crystallites. However, an increase in temperature to 500°C and heating the sample in hydrogen for 2 h resulted again in the core-and-ring structure (Fig. 3q). This shape remained unchanged after each of two additional intervals of heating (Fig. 3r). Obviously, the response of the specimen is still sluggish. An increase in temperature to 600°C and heating for 2 h in hydrogen caused considerable extension of the crystallites accompanied by a breakup of the particles (Fig. 3s).

The oscillatory behavior is not confined to freshly deposited samples heated in hydrogen. This behavior is exhibited also during continued heating of the specimen in hydrogen, following alternate heating in hydrogen and oxygen.

When purified hydrogen is used, the shape alternation is no longer observed, instead, compact particles are formed. For these experiments, ultrahigh-pure hydrogen from the cylinder was purified further by passing it through a Deoxo unit (Englehard Industries) followed by a silica-gel column and then through a molecular sieve bed immersed in liquid nitrogen. Introduction of trace quantities of oxygen or moisture into the purified gas stream of H_2 caused the reappearance of the torus or of the core-and-ring structure.

DISCUSSION

Varghese *et al.* (*3*) reported that small amounts of hydrocarbon impurities in oxygen led to spurious oscillations during the oxidation of CO on alumina-supported platinum. Subsequently, Rajagopalan and Luss (*14*) reported that ppm quantities of hydrocarbon impurities in hydrogen or oxygen did not affect the oscillations observed during hydrogen oxidation on a platinum plate. We cannot comment on the role, if at all, of the hydrocarbons, which are probably present in traces in any purified gas. However, the electron diffraction indicates that the shape alternation is, in the present case, a result of the presence of traces of oxygen and/or moisture in the ultrahigh-pure hydrogen. As already noted, the alternation is not observed when the hydrogen is further purified. In fact, the observed alternation in shape could be expected from, and is in conformity with, some of the results in the literature (*15–19*). Indeed, previous studies of alternate oxidation and reduction of Pd and Ni crystallites supported on planar, nonporous, alumina substrates (*15, 16, 18*) indicated differences in crystallite shape

and structure under oxidizing and reducing conditions. Upon heating in oxygen, Pd crystallites extended considerably, the extension being accompanied by the formation of not-too distinct toroidal shapes, tearing, and fragmentation. Nickel exhibited even more pronounced shape changes, forming toroidal crystallites with a small remnant particle within the torus of each crystallite, during heating in oxygen. In addition, Rajagopalan *et al.* (*17*) noted that during hydrogen oxidation on Ni, Pd, and Pt wires or disks, the oxygen-to-hydrogen ratio necessary to produce oscillatory behavior was the lowest (0.01 to 0.1) for Ni, which forms the strongest oxide, and the highest for Pt, which forms the weakest oxide. These results suggest that the ratio of oxygen to hydrogen necessary to generate oscillations should be even smaller for Fe than for Ni, since Fe, being the most electropositive metal of the group VIII elements, has the highest affinity among these metals for oxygen. Indeed, in the present experiments, shape alternations were observed with hydrogen containing only parts per million oxygen. The shape alternation is a result of periodic oxidation of the crystallites by the contaminant oxygen followed by their partial reduction by hydrogen. The presence of a reactive support (alumina) contributes considerably to the process. Electron diffraction indicated that the shape alternation is indeed associated with the oxidation followed by partial reduction of the catalyst. It is to be expected that the observed shape alternations will be accompanied by oscillations in effluent concentrations if the amount of catalyst will be sufficiently large. However, our experiments involve too small an amount of model catalyst for such oscillations to be detected. A possible explanation for the observed shape changes is described below.

As noted previously, the torus shape is associated with an oxidized state and the core-and-ring structure with a less-oxidized one. The micrographs indicate that the particles are extended in the oxidized state and

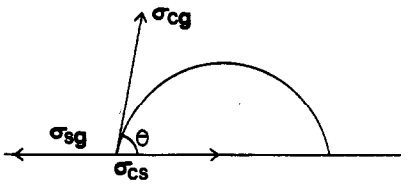

FIG. 4. Schematic of a particle in equilibrium on a substrate.

relatively contracted during the relatively reduced state. Such changes in the wetting characteristics are a consequence of the changes in the interfacial tensions and the resulting equilibrium which is expressed by Young's equation

$$\sigma_{cg} \cos \theta = \sigma_{sg} - \sigma_{cs},$$

where σ_{cg} is the interfacial tension between crystallite and gas, σ_{sg} is the interfacial tension between substrate and gas, σ_{cs} is the interfacial tension between crystallite and substrate, and θ is the wetting angle (Fig. 4). When the particle is oxidized, its σ_{cg} is smaller compared to the σ_{cg} of the metal. Also, due to the similarity of structures, the resulting iron oxide interacts more strongly with alumina than the metal does. As a result, the interfacial tension σ_{cs}, which decreases when the interaction energy U_{cs} between the crystallite and substrate increases, is smaller for the oxide than for the metal. The interfacial tension σ_{cs} is given by the expression

$$\sigma_{cs} = \sigma_c + \sigma_s - U_{cs},$$

where σ_c and σ_s are the surface tensions of the crystallite and substrate, respectively, when the gas phase is ignored (in general $\sigma_c \approx \sigma_{cg}$ and $\sigma_s \approx \sigma_{sg}$). Indeed, if the two surfaces could be placed in contact without any intermolecular interaction between the two, the interfacial tension would be equal to the sum of their surface tensions ($\sigma_c + \sigma_s$ in the present case). Since there are intermolecular interactions, the interfacial tension is obtained by subtracting from the above sum the interaction energy U_{cs} between the two bodies in contact. The de-

crease in σ_c and in σ_{cs} because of oxidation decreases the wetting angle θ and, as a result, the particle extends over the substrate to a new, smaller, equilibrium angle.

In the case of iron on alumina, the crystallites formed initially by vaporization are oxidized and hence tend to extend on the substrate. In addition, the chemical interaction between iron oxide and alumina (leading to the formation of a compound at the interface) can increase tremendously the value of U_{cs}, making σ_{cs} small or even negative (σ_{cs} could be negative under nonequilibrium conditions; under equilibrium conditions $\sigma_{cs} \geq 0$). Such a drastic reduction in the dynamic interfacial tension σ_{cs} and also a decrease in the value of σ_{cg}, caused by oxidation, lead to a rapid spreading of the crystallite over the substrate since the driving force for spreading $\sigma_{sg} - \sigma_{cg} \cos \theta - \sigma_{cs}$ becomes very large. The torus, enclosing a cavity which still contains oxide, is formed during this process of rapid extension. This rapid extension is soon arrested, because the oxide has already dissolved into the substrate near the surface and the subsequent interaction energy U_{cs} at the interface between the aluminate and the oxide, which do not form a chemical compound, is no longer so large as that between alumina and the oxide, which do form such a compound. In other words, σ_{cs} increases and a tendency to reach an equilibrium angle is achieved. The oxide may continue to dissolve into the substrate, because the formation of aluminate decreases the free energy of the system. This process continues until the diffusional resistance becomes so large that the rate of dissolution of the oxide becomes almost zero. On continued heating, reduction occurs and Fe_2O_3 diffuses back into the cavity to be reduced, at least partially, to iron. Obviously, the reduction of the solid solution of Fe_2O_3 in Al_2O_3 present beneath the torus is a much slower process because of the shielding provided by the material of the torus. Reduction of the oxide increases σ_c and σ_{cs} and for reasons already explained, both the torus and the material in the cavity tend to contract. Since the oxide which diffused out into the cavity does not sinter completely with the torus, the tendency to contract detaches this material from the torus which is anchored to the substrate via aluminate. This leads to the gap formation and the core-and-ring structure. Subsequently, during oxidation, the core disappears, both because of the diffusion of the oxide into the substrate and the emission of molecules due to a Kelvin effect, and the torus shape forms again. (Since the core has a smaller radius of curvature than the torus and, also, the inner surface of the torus has a negative radius of curvature, there is a strong tendency for the molecules to be emitted from the core onto the torus.)

As noted in the previous section, the apparent sluggishness in the shape change of the crystallites after a long duration of heating of the sample in hydrogen is a result of the specifics of the supported model catalyst. Unlike the unsupported cases, the changes are not restricted to the surface of the crystallites, but complete structure changes occur as a result of their interaction with the support. Also sintering of the crystallites affects the process. The repeated changes in shape and structure "torture" the system and lead to mechanical fatigue and an eventual breakup of the crystallites, as shown in Figs. 3p and s. An increase in temperature to 500°C causes "healing," and a return to the previous shape (Fig. 3q). Nevertheless, the catalyst is still aged and therefore the response is still sluggish as evidenced by the marginal change in shape on further heating (Fig. 3r). Further increase in temperature to 600°C causes considerable extension, as a result of enhanced oxidation, and it is accompanied again by a breakup of the particles. Indication of the extension of the crystallites and interaction with the support, probably preceding the breakup, can be seen from the particle traces in the micrographs (Fig. 3t).

CONCLUSION

The present results show that during heating in hydrogen containing traces of oxygen, alternation in crystallite shapes occurs in model, alumina-supported, iron catalysts. The shape alternates between a torus enclosing a cavity and a torus separated by an annular gap from a core in the cavity. Such shape alternation is found to be associated with the alternating oxidation and partial reduction of the catalyst. The present results indicate that oscillations in effluent concentration could be associated with oxidized and relatively reduced surface states of the catalyst which in turn are associated with changes in shape. In addition, experiments show that, due to mechanical fatigue, the oscillations die down after prolonged heat treatment of the catalyst leading, finally, to the breakup of the particles. The present experiments demonstrate the utility of electron microscopy as an important supplementary tool in the study of oscillatory behavior in heterogeneous catalytic systems, since it provides information on the surface morphology and also on the chemical state of the catalyst (via electron diffraction).

REFERENCES

1. Sheintuch, M., and Schmitz, R. A., *Catal. Rev. Sci. Eng.* **15,** 107 (1977).
2. Slin'ko, M. G., and Slin'ko, M. M., *Catal. Rev. Sci. Eng.* **17,** 119 (1978).
3. Varghese, P., Carberry, J. J., and Wolf, E. E., *J. Catal.* **55,** 76 (1978).
4. Cutlip, M. B., and Kenney, C. N., *in* "Chemical Reaction Engineering-Houston" (V. W. Weekman and D. Luss, Eds.), ACS Symp. Ser. No. 65, p. 475. Amer. Chem. Soc., Washington, D. C., 1978.
5. Rathousky, J., Puszynski, J., and Hlavácek, V., *Z. Naturforsch. A* **35,** 1238 (1980).
6. Hlavácek, V., and Rathousky, J., *Chem. Eng. Sci.* **37,** 375 (1982).
7. Belyaev, V. D., Slin'ko, M. M., Slin'ko, M. G., and Timoshenko, V. I., *Dokl. Akad. Nauk. SSSR* **214,** 1098 (1974).
8. McCarthy, E., Zahradnik, J., Kuczynski, G. C., and Carberry, J. J., *J. Catal.* **39,** 29 (1975).
9. Eigenberger, G., *Chem. Eng. Sci.* **33,** 1263 (1978).
10. Schmitz, R. A., Renola, G. T., and Garrigan, P. C., *Ann. N. Y. Acad. Sci.* **326,** 638 (1978).
11. Kurtanjek, Z., Sheintuch, M., and Luss, D., *J. Catal.* **66,** 11 (1980).
12. Sault, A. G., and Masel, R. I., *J. Catal.* **73,** 294 (1982).
13. Chu, Y. F., and Ruckenstein, E., *J. Catal.* **55,** 281 (1978).
14. Rajagopalan, K., and Luss, D., *J. Catal.* **61,** 289 (1980).
15. Chen, J. J., and Ruckenstein, E., *J. Phys. Chem.* **85,** 1606 (1981); Ruckenstein, E., and Chen, J. J., *J. Colloid Interface Sci.* **86,** 1 (1982).
16. Ruckenstein, E., and Lee, S. H., *J. Catal.* **86,** 457 (1984).
17. Rajagopalan, K., Sheintuch, M., and Luss, D., *Chem. Eng. Commun.* **7,** 335 (1980).
18. Nakayama, T., Arai, M., and Nishiyama, Y., *J. Catal.* **79,** 497 (1983).
19. Tatarchuk, B. J., Chludzinski, J. J., Sherwood, R. D., Dumesic, J. A., and Baker, R. T. K., *J. Catal.* **70,** 433 (1981).